AXISYMMETRIC FLOW-INDUCED BIREFRINGENCE MEASUREMENTS FOR THE FLOW OF A POLYSTYRENE BOGER FLUID INTO AN ABRUPT CONTRACTION-EXPANSION

JONATHAN P. ROTHSTEIN & GARETH H. MCKINLEY

Department of Mechanical Engineering, M.I.T., 77 Massachusetts Ave., Cambridge, MA 02139, USA

ABSTRACT

We study the creeping flow of a dilute, monodisperse polystyrene/oligomeric styrene Boger fluid through axisymmetric abrupt contraction-expansions of various contraction ratios and over a wide range of Deborah numbers. Measurements of the entry pressure drop for the polystyrene solution increase monotonically with Deborah number and are substantially larger than those observed for a similar Newtonian fluid. Axisymmetric flow-induced birefringence measurements upstream of the 4:1:4 contraction-expansion show a region of strong polymer chain extension which increases in strength and in size with Deborah number. Downstream measurements reveal a region of axial compression whose size and position are independent of Deborah number.

INTRODUCTION

Recent measurements and Brownian dynamics simulations of the tensile stress growth and birefringence in transient uniaxial elongation of dilute polymer solutions have revealed the existence of a 'stress-conformation' hysteresis [1]. In a strong stretching flow, the average configuration and resulting stress in a polymer chain are found to evolve along quite different paths during stretching and relaxation. This hysteresis arises from non-equilibrium coupling between the macroscopic flow field and the internal degrees of freedom of the fluid microstructure, and provides an additional mechanism for dissipation of mechanical energy. To capture such effects, recent closed-form constitutive models have postulated the existence of an additional, purely-dissipative internal contribution to the polymeric stress [2] which can at least qualitatively capture the rapid changes in stress observed in Brownian dynamics simulations[3]. The consequences of this molecular-level hysteresis on the macroscopic characteristics of a complex flow have never been investigated. In the present work, we study a prototypical transient extensional flow: the motion of a viscoelastic fluid through an abrupt axisymmetric contraction-expansion with various contraction ratios. A schematic diagram of the axisymmetric contraction-expansion is shown in Figure 1. The fluid experiences shear near the walls, uniaxial extension along the centerline upstream of the contraction plane (z=0) and biaxial expansion downstream of the re-expansion ($z = 2R_2$).

The test fluid is a well-characterized dilute (0.025wt%) polymer solution of monodisperse polystyrene (M_w=2x10^{6}g/mol) dissolved in oligomeric styrene. A complete discussion of the rheology of the test fluid can be found in Rothstein and McKinley (1999) [4].

Experimental pressure drop measurements across a 4:1:4 contraction-expansion have shown a substantial extra pressure drop above the value observed for a similar Newtonian fluid at the same flow rate [4]. This viscoelastic enhancement of the dimensionless pressure drop is *not* associated with the onset of an elastic or an inertial flow instability. However, it is not qualitatively predicted by existing steady-state or transient numerical computations with simple dumbbell models. The failure of these constitutive models to predict the correct evolution of macroscopic properties of complex flows with Deborah number may be due to an inadequate description of the microscopic deformation. To investigate the microstructural dynamics of the polystyrene molecule, we have utilized the axisymmetric flow-induced birefringence (FIB) technique of Li and Burghardt [5].

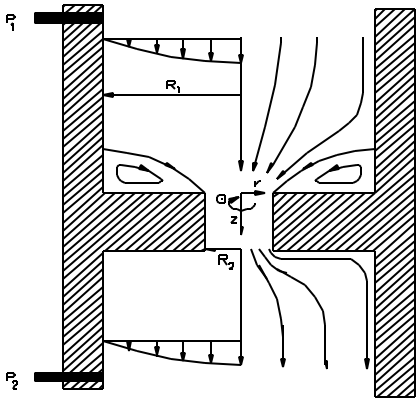

Figure 1: Schematic diagram of an axisymmetric abrupt contraction- expansion. The contraction ratio is R_1/R_2.

The molecular polarizability (and hence the macroscopic refractive index) of a polymer chain is different in the direction parallel to and normal to the chain backbone [6]. Flow-induced birefringence utilizes this refractive index mismatch to probe the microscopic deformation of polymer chains. The optical path for the polarization modulated flow birefringence system employed in this research is shown in Figure 2.

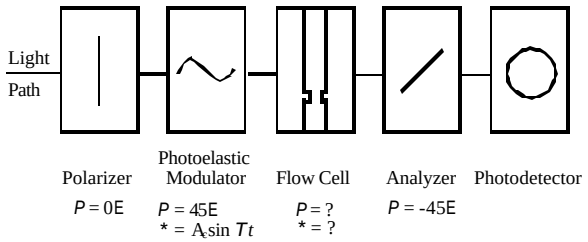

Figure 2: Optical path employed to measure polarization modulated axisymmetric flow birefringence.

By passing light of a known polarization state and frequency through the polymeric fluid in the flow cell and measuring the resulting change in polarization state, flow-induced birefringence can be used to determine the local anisotropy in the conformation of the polymer chains

$$\frac{\Delta n'}{C} = \nu k_B T \Delta A, \qquad (1)$$

where ΔnN is the measured birefringence, C is the *stress-optical coefficient*, $\Delta A = A_{||} - A_z$ is a measure of the anisotropy in the average conformation of the polymer chain and the elastic modulus is $G = n k_B T \Delta A$. The polymer conformation is characterized by the second order tensor, $\mathbf{A} = \langle \mathbf{QQ} \rangle$, where $\mathbf{Q}$ is the end-to-end vector of the polymer chain. The intensity the light entering the photodetector is given by:

$$I(t) = I_{dc}[1 + 2J_1(A_c)M_{34}\sin\omega t + 2J_2(A_c)M_{32}\cos 2\omega t], \quad (2)$$

where the components of the Mueller matrix $M_{32} = [1 - \cos\delta]\sin 2\chi \cos 2\chi$ and $M_{34} = \sin\delta \cos 2\chi$ correspond to the optical train shown in Figure 2. From these measurements it is possible to calculate both the retardation, $\delta = (2\pi \Delta n' d)/\lambda$, and the extinction angle, c, simultaneously, where d is the path length of the light through the birefringent media and l is the wavelength of the laser.

$$\delta = \cos^{-1}\left(\frac{-M_{32}^2 \pm \sqrt{1 - M_{34}^2 - M_{32}^2}}{M_{34}^2 + M_{32}^2} \right),$$
$$\chi = \frac{1}{2}\cos^{-1}\left(\frac{M_{34}}{\sin\delta} \right). \qquad (3)$$

Flow-induced birefringence has typically been used only in two-dimensional flows of polymer melts and solutions because it is a line-of-sight technique. In the flow through an axisymmetric geometry such as the contraction-expansion, the kinematics and the molecular conformation and subsequently the anisotropic conformation vary along the path of the light resulting in an integrated measure of the flow-induced birefringence

$$I_1 = \int \sin\delta \cos 2\chi \, dl,$$
$$I_2 = \int [1 - \cos\delta]\sin 2\chi \cos 2\chi \, dl, \qquad (4)$$

where l is the path of the light through the birefringent material [5]. Deconvoluting local measures of $\delta(r,z)$ and $\chi(r,z)$ from integral measures is ill-posed; however, numerical simulations can be used to compare measured and computed values of I_1 and I_2 directly [7].

RESULTS

A comparison of the dimensionless pressure drop

$$P = \frac{\left[P_2 - P_1 - \Delta P_{Poiseuille}\right]_{non-Newtonian}}{\left[P_2 - P_1 - \Delta P_{Poiseuille}\right]_{Newtonian,\,4:1:4}} = \frac{\Delta P(De \neq 0)}{\Delta P_{4:1:4}(De = 0)}, \quad (5)$$

for several contraction ratios is shown in Figure 3, where the pressures P_1 and P_2 are measured using the flush mounted transducers shown in Figure 1. In each case, the pressure drop is equal to that of a Newtonian fluid at low Deborah numbers. As the Deborah number is increased, the dimensionless pressure drop begins to monotonically increase with Deborah number. At a higher critical Deborah number, the flow becomes unstable and the axisymmetry is broken. These trends have been observed previously in the case of the 4:1:4 contraction-expansion[4].

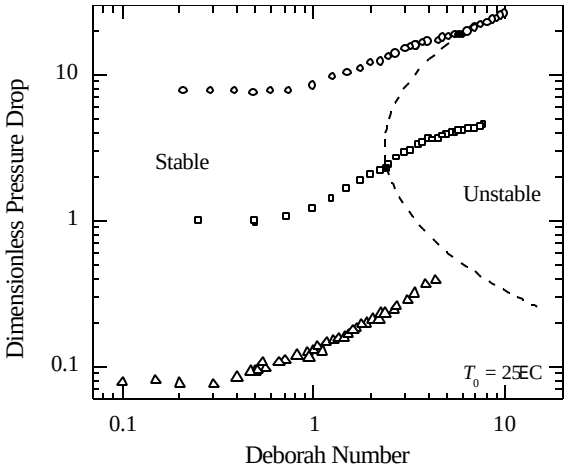

Figure 3: Dimensionless pressure drop for the 2:1:2 (Î), 4:1:4 (~) and 8:1:8 contraction-expansions (•).

The flow cell in Figure 2 used for FIB measurements was created by boring a circular hole through a block of low birefringence glass (Schott BK7). To establish a seal between the flow cell and upstream and downstream tubing, the glass was held under constant compression within an aluminum superstructure. This induced compressive stress coupled with the pressure developed under flow condition results in a parasitic birefringence within the flow cell. The integrated ratios I_1 and I_2 are therefore due not only to the flow-induced birefringence, but also to the parasitic birefringence of the glass. To calculate the retardation and extinction angle of the fluid, it is necessary to first determine the compressive and pressure induced birefringence and then to systematically remove them from the flow signals. If the retardation of any of three birefringence signals is large, this process can

be a very difficult exercise in Mueller calculus. However, if the retardation is assumed small, then the contribution to the total birefringence signals of each component (flow, pressure and compressive) simply become additive

$$I_1 = \delta_c \cos 2\chi_c + \delta_p \cos 2\chi_p + \delta'_{FIB} \cos 2\chi'_{FIB}. \qquad (6)$$

In this case, the primes indicate quantities that have been integrated along the path of the incident beam.

In Figure 4, the procedure for systematically removing the pressure and compressive contributions to the total I_1 signal is demonstrated for the axisymmetric flow-induced birefringence measurements taken at a Deborah number of De = 4.0 along the centerline upstream of the contraction plane ($z < 0$).

Due to a strong mismatch in the indices of refraction between the flow cell glass and the polystyrene Boger fluid, curvature effects make it possible to take FIB measurements only along the centerline ($r = 0$). One of the consequences of this limitation is that the extinction angle of the polymer chains is always oriented along the z axis.

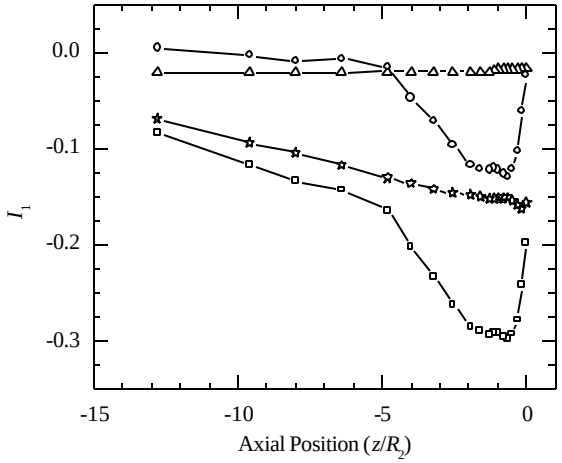

Figure 4: Contribution of compressive stress ( ), pressure ( ) and flow-induced birefringence (•) to the total I_1 signal (~) measured along the upstream centerline at a De = 4.0.

In Figure 5, the retardation upstream of the 4:1:4 contraction-expansion is shown at several Deborah numbers. For low Deborah numbers, the retardation is immeasurably small. The deformation due to shear near the walls is not significant enough at these flow rates to be observed over the signal noise. As the Deborah number is increased, the shear deformation caused by radial inflow along the plane of the contraction results in axial compression of the polymer conformation ($d > 0$) at small distances upstream ($z/R_2 < !1$). At large Deborah numbers ($De > 1$), extension of the polymer chains ($d < 0$) due to the strong extensional flow along the centerline is observed further upstream of the contraction plane (z/R_2 - !5). The increase in magnitude and upstream influence of the chain radial elongation is observed to occur concurrently with the growth and development of the corner vortex[4].

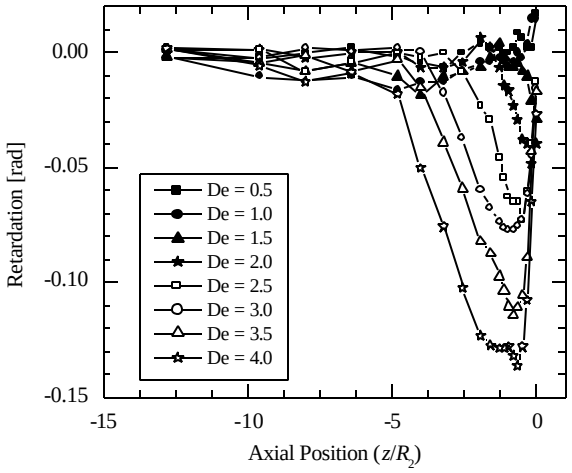

Figure 5: Retardation measurements along the centerline upstream of a 4:1:4 axisymmetric contraction-expansion

The retardation along the centerline downstream of the axisymmetric contraction-expansion is shown in Figure 6 for a large range of Deborah numbers. At low Deborah numbers, the fluid retardation is again essentially zero. As the Deborah number is increased a region of compression is observed roughly one contraction radius downstream of the re-expansion (z/R_2 . 3). Note that the throat is of length $L_c = 2R_2$. This compression results from the biaxial expansion of the fluid as it suddenly decelerates out of the contraction and its magnitude and position are independent of Deborah number. As the Deborah number is increased, the strong extensional flow upstream of the contraction coupled with the shear flow within the contraction produces a region of extension just downstream of the re-expansion plane.

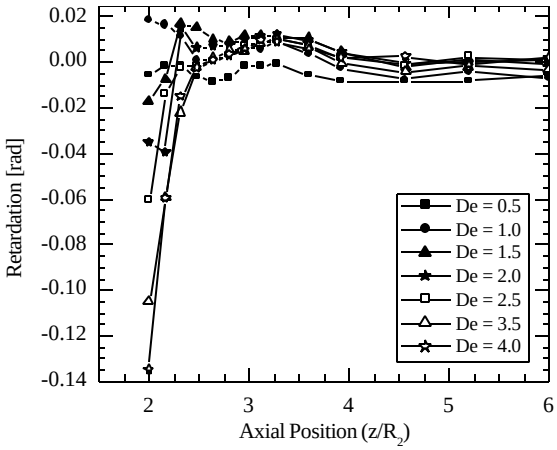

Figure 6: Retardation measurements along the centerline downstream of a 4:1:4 axisymmetric contraction-expansion

CONCLUSIONS

This research couples macroscopic measurements of the effects of viscoelasticity (enhanced pressure drop and flow stability) with microscopic conformation measurements (axisymmetric flow-induced birefringence) of

a well characterized dilute monodisperse polymer solution (PS/PS Boger fluid) in a prototypical complex flow (4:1:4 contraction-expansion). These measurements provide a comprehensive data set for the validation of constitutive equations and numerical methods.

REFERENCES

1. P. S. Doyle, E. S. G. Shaqfeh, G. H. McKinley and S. H. Spiegelberg, *J. Non-Newtonian Fluid Mech.* 76 (1998) 79-110.
2. J. M. Rallison, *J. Non-Newtonian Fluid Mech.* 68 (1997) 61-83.
3. L. Li and R. G. Larson, *Macromolecules* 33 (2000) 1411-1415.
4. J. P. Rothstein and G. H. McKinley, *J. Non-Newtonian Fluid Mech.* 86 (1999) 61-88.
5. J.-M. Li and W. R. Burghardt, *J. Rheol.* 39 (1995) 743-766.
6. G. G. Fuller, "*Optical Rheometry of Complex Fluids*", Oxford University Press, New York, (1995).
7. J.-M. Li, W. R. Burghardt, B. Yang and B. Khomami, *J. Non-Newtonian Fluid Mech.* 74 (1998) 151-193.